Arbitrary Polarization Conversion by the Photonic Band Gap of the One-Dimensional Photonic Crystal

Minjia Zheng, Jiajun Wang, Xingqi Zhao, Tongyu Li, Xiaohan Liu, and Lei Shi

***Abstract*— We demonstrate that an all-dielectric one-dimensional photonic crystal (1DPC) serves as an effective tool for arbitrary polarization conversion. Within the photonic band gaps (PBGs) of the 1DPC, perfect total reflection can be achieved. Under oblique incidence, the trends of reflection phase changes for p- and s-polarization within the PBGs are different. As the incident angle increases, the range of phase difference between p- and s-components gradually expands to $(0, 2\pi)$. When light is incident with a specific polarization state, the phase difference between the p- and s-components leads to the polarization conversion of the reflected light within the PBGs. By changing the polarization direction of the incident light, arbitrary polarization state conversion covering the full Poincaré sphere can be achieved. The efficiency of this conversion can reach 100% due to the perfect reflection within the PBGs and the non-absorptive nature of the all-dielectric 1DPC.**

***Index Terms*— Photonic crystals, one-dimensional photonic crystals, polarization conversion.**

I. Introduction

POLARIZATION is one of the intrinsic properties of transverse waves, especially electro-magnetic waves. Polarized light is crucial in diverse applications, such as optical communications, polarization imaging and nonlinear optics [1], [2], [3], [4], [5]. Conventional approaches to polarization modulation involve leveraging the birefringence properties of crystalline materials to introduce a phase delay between orthogonal polarization components of light [6]. Recently, great interests has been aroused in developing polarization control by using artificial micro/nano structures. Arbitrary polarization state conversion is achieved by the design of a variety of optical structures such as metasurfaces and photonic crystal slabs [7], [8], [9], [10], [11], [12], [13], [14], [15], [16]. Local resonances supported by metasurfaces can perform polarization-anisotropic phase and amplitude modulations, hence various polarization conversion can be realized by designing metasurfaces with different structural parameters [7], [8], [9], [10], [11]. For the structure of photonic crystal slabs, the arbitrary polarization control is strongly related to the guided resonance of band structures. For example, the complete polarization conversion between linear polarizations can be realized [12], [13], [14]. Besides photonic bands, photonic band gaps (PBGs) also show the powerful ability of light field modulations, though their ability of polarization modulations has not been sufficient studied yet.

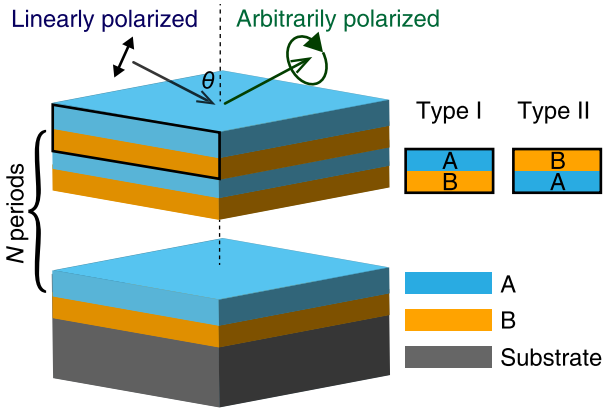

Fig. 1. Schematic of a 1DPC for arbitrary polarization state conversion. The 1DPC consists of N periods of two kinds of materials A and B with different refraction indices. There are two types of unit cells of the 1DPC and they can be configured as (AB) or (BA). When a linearly polarized light obliquely incident on the 1DPC, the polarization state of the reflected light will be converted to arbitrarily polarized by the 1DPC.

A one-dimensional photonic crystal (1DPC) is constructed by periodically alternating layers of materials with different refractive index. The structure of a 1DPC is shown in Fig. 1, consisting of two materials of A and B. The resulting periodic variation in the refractive index can lead to the creation of one-dimensional PBGs, which prevents the light's propagation [17]. The topological phases and edge states were found in 1D systems which are applicable of designing systems with interface states [18], [19]. Special material design can extend the applications of the total reflection PBGs to a wider range of incident angles [20], [21]. Though, applications using the reflection phase within the PBGs still deserve discovering.

Manuscript received 6 November 2023; revised 20 December 2023; accepted 23 January 2024. Date of publication 26 January 2024; date of current version 7 February 2024. This work was supported in part by the National Key Research and Development Program of China under Grant 2022YFA1404800 and Grant 2023YFA1406900; in part by the National Natural Science Foundation of China under Grant 12221004, Grant 12234007, and Grant 12321161645; in part by the Major Program of National Natural Science Foundation of China under Grant T2394481; and in part by the Science and Technology Commission of Shanghai Municipality under Grant 22142200400, Grant 21DZ1101500, Grant 2019SHZDZX01, and Grant 23DZ2260100. *(Corresponding authors: Jiajun Wang; Lei Shi.)*

Minjia Zheng, Jiajun Wang, Xingqi Zhao, Tongyu Li, and Xiaohan Liu are with the State Key Laboratory of Surface Physics, the Key Laboratory of Micro- and Nano-Photonic Structures (Ministry of Education), and the Department of Physics, Fudan University, Shanghai 200433, China (e-mail: jiajunwang@fudan.edu.cn).

Lei Shi is with the State Key Laboratory of Surface Physics, the Key Laboratory of Micro- and Nano-Photonic Structures (Ministry of Education), the Department of Physics, and the Institute for Nanoelectronic Devices and Quantum Computing, Fudan University, Shanghai 200433, China, also with the Collaborative Innovation Center of Advanced Microstructures, Nanjing University, Nanjing 210093, China, and also with the Shanghai Research Center for Quantum Sciences, Shanghai 201315, China (e-mail: lshi@fudan.edu.cn).

Color versions of one or more figures in this letter are available at https://doi.org/10.1109/LPT.2024.3358815.

Digital Object Identifier 10.1109/LPT.2024.3358815

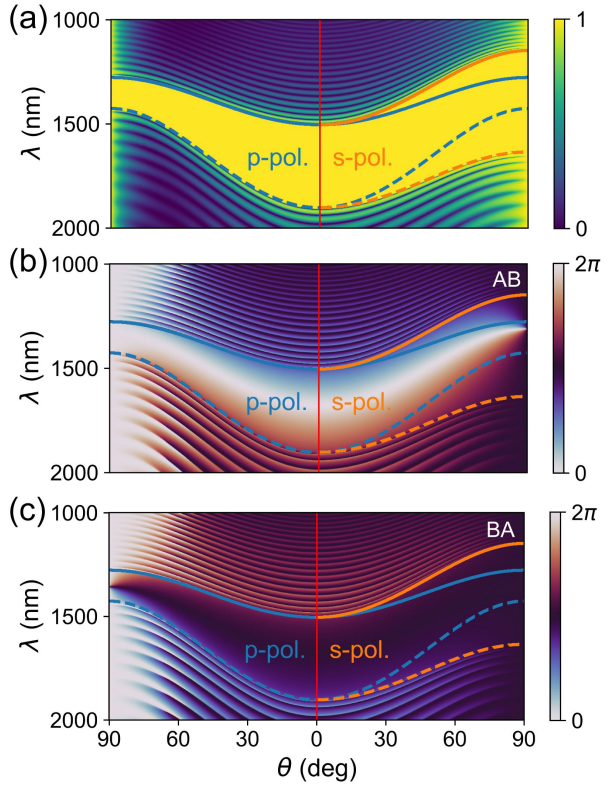

Fig. 2. (a) Reflection spectra of the designed 1DPC. The PBG is shown between the solid and dashed lines. The PBG for s-pol. (orange lines) is broadened, while the one for p-pol. (blue lines) narrows with respect to θ. The red line represents the case of normal incidence. Reflection phase spectra of the 1DPC with the unit cell of (b) (AB) and (c) (BA) are also shown. The edges of the PBG are also annotated in (b) and (c). For p-pol., the range of phase values within the PBG gradually narrows around 0 with the unit cell of (AB) while the range widens with the unit cell of (BA). For p-pol., the range of phase values within the PBG gradually widens around 0(or 2π) with the unit cell of (AB) while the range narrows with the unit cell of (BA).

In this Letter, we introduce a new approach based on an all-dielectric 1DPC for arbitrary polarization conversion. The PBG can be characterized as the perfect reflection, and its modulation of light can be divided into two orthogonal components which are considered as p- and s-polarization (p- and s-pol.). The PBGs under p- and s-polarized incidence show differences when the incidence is not normal. When oblique incidence is considered, due to the continuity of the electric field at boundaries of different media, there will be a phase difference between the reflected light for p- and s-pol. components. When an polarized light obliquely incident on the 1DPC within its PBG, it can modulate the phase differences of p- and s-components separately and the polarization state of the reflected light can be altered. This conversion can encompass a single trajectory of the Poincaré sphere. With changing the linear polarization direction of the incident light, the 1DPC can work as a full Poincaré sphere converter. Due to the perfect reflection within the PBGs and the non-absorptive nature of an all-dielectric 1DPC, the efficiency of this conversion can reach 100%.

II. Methods

The polarization state conversion can be implemented by an optical structure of 1DPC. We consider a 1DPC structure as is shown in Fig. 1. The structure consists of a periodic arrangement with two kinds of dielectric materials, denoted as A and B, each possessing different refraction indices, represented as n_A and n_B. The refractive indices of the external medium and the substrate are represented as n_0 and n_s. In this Letter, we present $n_A = 1.45$, $n_B = 2.1$, $n_0 = 1$ and $n_s = 1.52$ while the thickness of the two layers are $d_A = 289.7$ nm and $d_B = 200$ nm, respectively. Our 1DPC structure is designed for $N = 30$ periods of unit cells. Here, we consider two types of unit cells, which are (AB) and (BA).

By using the transfer matrix method, the reflection and phase spectra of the 1DPC structure of $(AB)^{30}$ for both p- and s-pol. are depicted in Fig. 2. The band structure of a 1DPC consists of two wavelength regions: one is the total reflection region, namely the PBG region(between the solid and dashed lines), and the other is the non-total reflection region, which is the photonic band region. The edges of the PBG are depicted by blue and orange lines for p- and s-pol., respectively. When $\theta = 0$, the reflectance for both s- and p-pol. are equivalent in the PBG. As the incident angle increases, the PBG for s-pol. is broadened, while the PBG for p-pol. narrows, which is attributed to Brewster effect.

The phase spectra of the 1DPC are depicted in Fig. 2(b) and (c) for both types of unit cells which are (AB) and (BA). As is shown in Fig. 2(b), when θ is degree, the phase distributions of p- and s-pol. are the same for the unit cell of (AB). As θ increases, for p-pol., the range of phase values within the PBG gradually narrows around 0(or 2π) while for s-polarzation, the range widens to cover a 2π range. On the contrary, in Fig. 2c, as θ increases, for p-pol., the range of phase values within the PBG gradually widens while for s-pol., the range narrows around π.

Furthermore, in Fig. 3, we show the reflection phase at the PBG's upper and lower edge of 1DPC for both p- and s-pol. Since the PBG is broadened for s-pol. with respect to θ, the PBG is only considered where the total reflectance is exhibited for both p- and s-pol. at the same θ and λ. In Fig. 3(a), for the unit cell of (AB), the difference of reflection phase at the upper and lower edges of the PBG for p-pol., denoted as $\phi_{p,\text{edge}}$, decreases from a specific value to 0, while the difference for s-pol., denoted as $\phi_{s,\text{edge}}$, eventually increases to an approximate value of 2π as θ increases. Because the PBG for p-pol. is narrower than the one for s-pol., $\phi_{s,\text{edge}}$ is slightly smaller than 2π for the unit cell of (AB). In Fig. 3(b), for the unit cell of (BA), $\phi_{s,\text{edge}}$ decreases to 0 while $\phi_{p,\text{edge}}$ increases to 2π. For this type of unit cell, $\phi_{p,\text{edge}}$ in overlapped PBGs for both p- and s-pol. can reach 2π. Based on this, to achieve arbitrary polarization conversion, we employ the 1DPC with a unit cell of (BA) into this work.

Here, to give an example, we consider the polarization conversion under the condition of linearly polarized incidence. We apply Jones vector to describe the incident light $\mathbf{E}_\text{i}$ and it can be written as

$$\mathbf{E}_\text{i} = \frac{1}{\sqrt{|E_p|^2 + |E_s|^2}} \begin{pmatrix} E_p \\ E_s \end{pmatrix}, \tag{1}$$

where E_p and E_s are the electric fields in the p- and s- directions, respectively. The Jones matrix $\mathbf{J}$, which describes

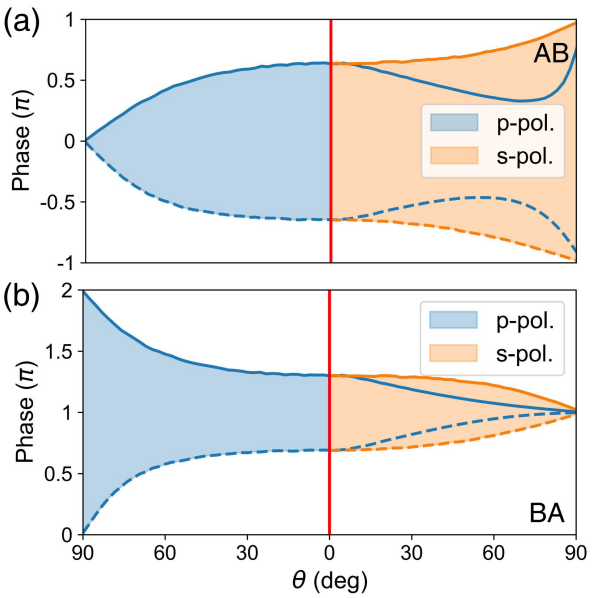

Fig. 3. Reflection phase of the designed 1DPC at the upper and lower edges of the PBG with respect to θ for the unit cell of (a) (AB) and (b) (BA). Blue area shows the phase range for p-pol. while orange area shows the range for s-pol. (a) For the unit cell of (AB), $\phi_{p,\text{edge}}$ decreases to 0 and $\phi_{s,\text{edge}}$ increases to approximately 2π and for the unit cell of (BA), $\phi_{p,\text{edge}}$ increases to 2π and $\phi_{s,\text{edge}}$ decreases to 0 with respect to θ. Blue lines in the orange area shows the reflection phase for s-pol. but at the PBG edges for p-pol. For arbitrary polarization conversion, blue lines are considered because the optical parameters remains unchanged with single incidence and the presence of PBG is mandatory for both p- and s-pol.

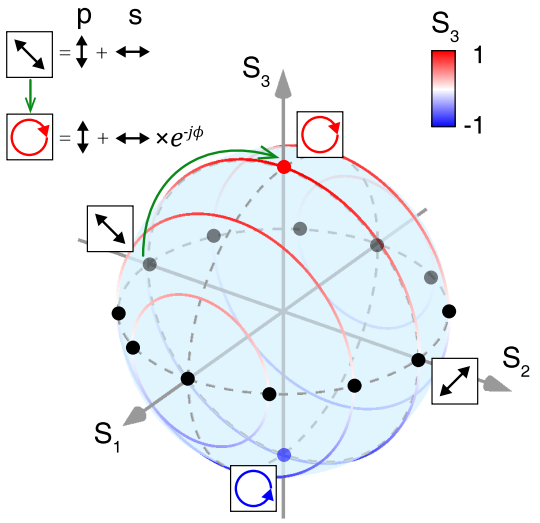

Fig. 4. Schematic of Poincaré sphere of the polarization conversion by a 1DPC with the unit cell of (BA). Any linearly polarized light (the circle where black dots are located) can be separated by p- and s-components. For instance, when a -45-degree linearly polarized light obliquely incident on the 1DPC, the reflected light will have a phase difference ϕ between p- and s-pol., which leads to the conversion of the polarization state (green arrow). Within the PBG, this conversion can encompass any point on the circle passing the black dot and has S_1 as its axis. When the linear polarization direction of the light varies, the circle also passes through the black dot representing the incident polarization and has S_1 as its axis.

the polarization modulation by the 1DPC, can be expressed as

$$\mathbf{J} = \begin{pmatrix} r_{pp} & r_{ps} \\ r_{sp} & r_{ss} \end{pmatrix}. \tag{2}$$

Because every plane across the normal line (black dashed line in Fig. 1) is the mirror plane of the 1DPC and the p- and s-components are orthogonal, 1DPC has no ability to convert the polarization direction of p- and s-polarized light, i.e., $r_{ps} = r_{sp} = 0$. An all-electric 1DPC is lossless and in its PBGs, total reflection occurs, which also means $|r_{pp}| = |r_{ss}| = 1$. r_{ss} can be replaced by $r_{pp} \cdot \exp(-j\phi)$, where ϕ is the reflection phase difference between the p- and s-components. So, the Jones vector of the reflected light $\mathbf{E}_r$ can be expressed as

$$\mathbf{E}_\text{r} = \mathbf{J} \times \mathbf{E}_\text{i} = \begin{pmatrix} r_{pp} & 0 \\ 0 & r_{pp}e^{-j\phi} \end{pmatrix} \times \frac{1}{\sqrt{|E_p|^2 + |E_s|^2}} \begin{pmatrix} E_p \\ E_s \end{pmatrix}. \tag{3}$$

For instance, $r_{pp} = \exp(-j\phi_p)$ and an incident light with 45-degree polarization direction $(E_s = E_p)$ is considered, the above equation can be further calculated to obtain

$$\mathbf{E}_\text{r} = \frac{1}{\sqrt{2}} \begin{pmatrix} 1 \\ \exp(-j\phi) \end{pmatrix}. \tag{4}$$

When $\phi = 0$, the reflected light is also linearly polarized. And when $\phi = \pi/2$ or $\phi = -\pi/2$, the reflected light is right- or left-handed circularly polarized. As is discussed before, for a 1DPC with the unit cell of (BA), ϕ is within the range of $(-\pi, \pi)$. Consequently, within the PBG, 1DPC can provide the capability to achieve polarization state conversion from linear to any other polarization covering from the left- to right-handed circular.

Furthermore, to illustrate such phase state conversion by a 1DPC more vividly, we can map these polarization states onto the Poincaré sphere using the Stokes parameters, as shown in Fig. 4. Here, the corresponding Stokes parameters can be defined as $S_0 = |E_s|^2 + |E_p|^2$, $S_1 = |E_s|^2 - |E_p|^2$, $S_2 = 2|E_s E_p| \cos\phi$ and $S_3 = 2|E_s E_p| \sin\phi$. The polarization state can be described by normalized Stokes parameters $\mathbf{S} = (\frac{S_1}{S_0}, \frac{S_2}{S_0}, \frac{S_3}{S_0})$. In Fig. 4, the polarization conversion process is visually depicted on the surface of Poincaré sphere. We have demonstrated that for the incidence of a 45-degree linearly polarized light, where $\mathbf{S} = (0, \pm 1, 0)$, the polarization state of reflected light can be converted to circular or elliptical in the PBG and this conversion can be mapped onto the circle passing the four poles where $S_3 = \pm 1$ and $S_2 = \pm 1$. Moreover, for any polarization state on this trajectory, it is feasible to decompose it into p- and s-components, when the polarized light is obliquely incident upon the 1DPC, the range of the phase difference ϕ between p- and s- components remains to be $(-\pi, \pi)$. This means that when the polarization state of the incident light is positioned anywhere along this trajectory, the one of the reflected light can also reach any point on the same circle. From the perspective of geometric phase, p- and s-pol. can be treated as two orthogonal eigen-polarizations. If these two polarization states are considered as the north and south poles of the Poincaré sphere, the 1DPC can achieve arbitrary polarization conversions along the same latitude [22], [23]. When the light is normally incident onto the 1DPC where the p- and s-pol. cannot be well defined, 1DPC shows no capability of arbitrary polarization state conversion.

To give an example, the polarization conversion is depicted in Fig. 4 (green arrow) which is between two polarization states expressed as $\mathbf{S} = (0, -1, 0)$ and $\mathbf{S} = (0, 0, 1)$. Here, the ellipticity and azimuth of the initial polarization state of the incident light are 0 and $-\pi/4$, respectively. The polarization conversion can be induced by the $\pi/2$ reflection phase difference between p- and s-pol. Since this phase difference within the PBG of the 1DPC can cover the range from 0 to 2π, we can fix the incident wavelength and polarization, and adjust θ to a suitable value, ensuring that the reflection phase difference are precisely equal to $\pi/2$. The polarization state of the reflected light will be converted to $\mathbf{S} = (0, 0, 1)$. Here, the ellipticity of the polarization of the signal is $\pi/4$ and the azimuth of it is cannot be defined at that point. This operation will change the ellipticity of the incident light. In Fig. 4, some other trajectories representing the polarization conversion are also depicted. To achieve more conversion, we can simply control the polarization direction of linear polarized incident light, which means changing the ratio of E_p to E_s in Eq. (3). For the incidence of these linear polarization states whose S_1 components are fixed, the reflected polarization states can reach any point on the trajectories where S_1 components remain to be unchanged. Consequently, for any polarization state of the incident light, 1DPC can provide arbitrary polarization state conversion covering the full Poincaré sphere within its PBG.

III. Conclusion

To conclude, we found that the reflection phase difference of the 1DPC within its PBG between p- and s-pol. The phase difference covers the range of $(-\pi, \pi)$ for the unit cell of (BA) where $n_B > n_A$. For any polarized incident light, 1DPC shows the ability to convert the polarization state of the reflected light. This conversion moves along the trajectory where S_1 component is fixed. By changing the polarization direction of the incident light, the polarization conversion by the 1DPC can cover the full Poincaré sphere within its PBG. Due to the perfect reflection within the PBG of an all-dielectric 1DPC, this lossless structure makes the efficiency of this polarization conversion to 100%. This approach merely requires media with different refractive indices. It is a straightforward design that can be employed in the creation of optical components to meet specific polarization conversion requirements.

References

[1] Z.-Y. Chen et al., "Use of polarization freedom beyond polarization-division multiplexing to support high-speed and spectral-efficient data transmission," *Light, Sci. Appl.*, vol. 6, no. 2, Aug. 2016, Art. no. e16207.

[2] N. A. Rubin, G. D'Aversa, P. Chevalier, Z. Shi, W. T. Chen, and F. Capasso, "Matrix Fourier optics enables a compact full-Stokes polarization camera," *Science*, vol. 365, no. 6448, Jul. 2019, Art. no. eaax1839.

[3] H. Hu, Q. Gan, and Q. Zhan, "Generation of a nondiffracting superchiral optical needle for circular dichroism imaging of sparse subdiffraction objects," *Phys. Rev. Lett.*, vol. 122, no. 22, Jun. 2019, Art. no. 223901.

[4] G. Li et al., "Continuous control of the nonlinearity phase for harmonic generations," *Nature Mater.*, vol. 14, no. 6, pp. 607–612, Apr. 2015.

[5] N. Segal, S. Keren-Zur, N. Hendler, and T. Ellenbogen, "Controlling light with metamaterial-based nonlinear photonic crystals," *Nature Photon.*, vol. 9, no. 3, pp. 180–184, Feb. 2015.

[6] M. Born and E. Wolf, *Principles of Optics: Electromagnetic Theory of Propagation, Interference and Diffraction of Light*. Amsterdam, The Netherlands: Elsevier, 2013.

[7] R. C. Devlin, A. Ambrosio, N. A. Rubin, J. P. B. Mueller, and F. Capasso, "Arbitrary spin-to-orbital angular momentum conversion of light," *Science*, vol. 358, no. 6365, pp. 896–901, Nov. 2017.

[8] J. Hao et al., "Manipulating electromagnetic wave polarizations by anisotropic metamaterials," *Phys. Rev. Lett.*, vol. 99, no. 6, Aug. 2007, Art. no. 063908.

[9] C. Huang, Y. Feng, J. Zhao, Z. Wang, and T. Jiang, "Asymmetric electromagnetic wave transmission of linear polarization via polarization conversion through chiral metamaterial structures," *Phys. Rev. B, Condens. Matter*, vol. 85, no. 19, May 2012, Art. no. 195131.

[10] Y. Yang, W. Wang, P. Moitra, I. I. Kravchenko, D. P. Briggs, and J. Valentine, "Dielectric meta-reflectarray for broadband linear polarization conversion and optical vortex generation," *Nano Lett.*, vol. 14, no. 3, pp. 1394–1399, Feb. 2014.

[11] S. Wang et al., "Arbitrary polarization conversion dichroism metasurfaces for all-in-one full Poincaré sphere polarizers," *Light, Sci. Appl.*, vol. 10, no. 1, p. 24, Jan. 2021.

[12] F. Chen et al., "Observation of topologically enabled complete polarization conversion," *Laser Photon. Rev.*, vol. 17, no. 4, Jan. 2023, Art. no. 2200626.

[13] Y. Guo, M. Xiao, Y. Zhou, and S. Fan, "Arbitrary polarization conversion with a photonic crystal slab," *Adv. Opt. Mater.*, vol. 7, no. 14, Jan. 2019, Art. no. 1801453.

[14] Y. Guo, M. Xiao, and S. Fan, "Topologically protected complete polarization conversion," *Phys. Rev. Lett.*, vol. 119, no. 16, Oct. 2017, Art. no. 167401.

[15] A. H. Gevorgyan et al., "Polarization plane's weak rotation amplifiers and polarization azimuth stabilizers," *Optik*, vol. 117, no. 7, pp. 309–316, Jul. 2006.

[16] A. H. Gevorgyan and S. S. Golik, "Optics of helical periodical media with giant magneto-optical activity," *Opt. Laser Technol.*, vol. 149, May 2022, Art. no. 107810.

[17] J. D. Joannopoulos et al., *Photonic Crystals: Molding the Flow of Light*, 2nd ed. Princeton, NJ, USA: Princeton Univ. Press, 2008.

[18] M. Xiao, Z. Q. Zhang, and C. T. Chan, "Surface impedance and bulk band geometric phases in one-dimensional systems," *Phys. Rev. X*, vol. 4, no. 2, Apr. 2014, Art. no. 021017.

[19] W.-M. Deng et al., "Ideal nodal rings of one-dimensional photonic crystals in the visible region," *Light, Sci. Appl.*, vol. 11, no. 1, p. 134, May 2022.

[20] F. Wu et al., "Redshift gaps in one-dimensional photonic crystals containing hyperbolic metamaterials," *Phys. Rev. Appl.*, vol. 10, no. 6, Dec. 2018, Art. no. 064022.

[21] G. Lu et al., "Perfect optical absorbers in a wide range of incidence by photonic heterostructures containing layered hyperbolic metamaterials," *Opt. Exp.*, vol. 27, no. 4, pp. 5326–5336, Feb. 2019.

[22] S. Ramaseshan, "The Poincaré sphere and the pancharatnam phase-some historical remarks," *Current Sci.*, vol. 59, pp. 1154–1158, Nov. 1990.

[23] M. V. Berry, "Pancharatnam, virtuoso of the Poincaré sphere: An appreciation," *Current Sci.*, vol. 67, pp. 220–223, Aug. 1994.